HHS Public Access

Author manuscript

Biochim Biophys Acta Mol Basis Dis. Author manuscript; available in PMC 2019 April 30.

Published in final edited form as:

Biochim Biophys Acta Mol Basis Dis. 2018 September ; 1864(9 Pt B): 2761–2768. doi:10.1016/j.bbadis.2018.05.001.

Blockade of TREM-1 prevents vitreoretinal neovascularization in mice with oxygen-induced retinopathy

Modesto A. Rojas[a,*], **Zu T. Shen**[b], **Ruth B. Caldwell**[a,c], and **Alexander B. Sigalov**[b,*]

[a]Vascular Biology Center, Augusta University, Augusta, GA 30912, United States

[b]SignaBlok, Inc, P.O. Box 4064, Shrewsbury, MA 01545, United States

[c]Charlie Norwood VA Medical Center, Augusta, GA 30904, United States

Abstract

In pathological retinal neovascularization (RNV) disorders, the retina is infiltrated by activated leukocytes and macrophages. Triggering receptor expressed on myeloid cells 1 (TREM-1), an inflammation amplifier, activates monocytes and macrophages and plays an important role in cancer, autoimmune and other inflammation-associated disorders. Hypoxia-inducible TREM-1 is involved in cancer angiogenesis but its role in RNV remains unclear. Here, to close this gap, we evaluated the role of TREM-1 in RNV using a mouse model of oxygen-induced retinopathy (OIR). We found that hypoxia induced overexpression of TREM-1 in the OIR retinas compared to that of the room air group. TREM-1 was observed specifically in areas of pathological RNV, largely colocalizing with macrophage colony-stimulating factor (M-CSF) and CD45- and Iba-1-positive cells. TREM-1 blockade using systemically administered first-in-class ligand-independent TREM-1 inhibitory peptides rationally designed using the signaling chain homooligomerization (SCHOOL) strategy significantly (up to 95%) reduced vitreoretinal neovascularization. The peptides were well-tolerated when formulated into lipopeptide complexes for peptide half-life extension and targeted delivery. TREM-1 inhibition substantially downregulated retinal protein levels of TREM-1 and M-CSF suggesting that TREM-1-dependent suppression of pathological angiogenesis involves M-CSF. Targeting TREM-1 using TREM-1-specific SCHOOL peptide inhibitors represents a novel strategy to treat retinal diseases that are accompanied by neovascularization including retinopathy of prematurity.

[*]Corresponding authors. mrojas@augusta.edu (M.A. Rojas), sigalov@signablok.com (A.B. Sigalov).

Author contribution statement

M.A.R., Z.T.S., R.B.C. and A.B.S. contributed to the interpretation of the results and finalized the manuscript. M.A.R. and A.B.S. conceived and designed the experiments. M.A.R., Z.T.S. and A.B.S. performed the experiments. M.A.R., Z.T.S., R.B.C. and A.B.S. analyzed the data. M.A.R., Z.T.S., R.B.C. and A.B.S. wrote and modified the paper.

Conflict of interests

Alexander B. Sigalov and Zu T. Shen are employees of SignaBlok, Inc. No other author has a conflict of interest to disclose.

Transparency document

The Transparency document associated with this article can be found, in online version.

Supplementary data to this article can be found online at https://doi.org/10.1016/j.bbadis.2018.05.001.

Keywords

Triggering receptor expressed on myeloid cells 1; Neovascularization; SCHOOL model of cell signaling; TREM-1 peptide inhibitors; Retinopathy

1. Introduction

Pathological retinal neovascularization (RNV) causes an angiogenesis-related vision impairment in retinopathy of prematurity (ROP), diabetic retinopathy (DR), and retinal vein occlusion (RVO), which are the most common causes of vision loss and blindness in each age group [1–4]. In premature infants, normal retinal vascular development is interrupted resulting in retinal ischemia and invasion of the vitreous by abnormal neovessels. In addition, vitreoretinal neovascularization can promote traction retinal detachment, leading to blindness [5]. In the United States, 14,000–16,000 premature infants are affected by ROP annually [6,7]. Conventional therapeutic options include laser ablation and the anti-vascular endothelial growth factor (VEGF) therapy, which both have their limitations and complications. Laser therapy is often accompanied by corneal edema, anterior chamber reaction, intraocular hemorrhage, cataract formation, and intraocular pressure changes [4], while the VEGF-targeted therapy can be complicated by damage of healthy vessels, potential side effects on neurons, rapid vascular regrowth upon interrupting the VEGF blockade, and limited effectiveness in some patients [8–11]. This suggests an unmet need for new targeted therapies that can better address the pathogenesis of RNV diseases and improve their treatment.

Retinal microglia and blood-derived macrophages (BDM) play a key role in regulating angiogenesis in the retina and choroid and, as such, are critically involved in the pathogenesis of RNV diseases [12–16]. In the oxygen-induced retinopathy (OIR) mouse model [17] that is widely used to study the pathogenesis of RNV as well as to evaluate medical intervention for retinal angiopathies, the retina is infiltrated by activated leukocytes and macrophages, and retinal microglial cells show phenotypic changes that have been implicated in the vascular pathology [18]. While retinal microglia can become activated in response to retinal pathologies [19], infiltration and activation of BDM may provide a major contribution in retinal degeneration [20]. In mice with OIR, macrophages promote the development of pathological RNV [21]. Macrophages induce angiogenesis by secreting multiple pro-angiogenic factors, including VEGF [22], monocyte chemotactic protein 1 (MCP-1/ CCL2) [23] and cytokines, such as tumor necrosis factor-alpha (TNFα) and interleukin (IL)-1β [24]. In line with these studies, inhibition of MCP-1 has been shown to suppress RNV [25,26].

Triggering receptor expressed on myeloid cells-1 (TREM-1), an inflammation amplifier expressed predominantly on neutrophils and monocytes, plays a role in innate and adaptive immune responses [27–32], and is upregulated under a variety of inflammatory conditions [33–36]. Upon activation, TREM-1 enhances the production of multiple cytokines and growth factors including MCP-1, TNFα, IL-1α, IL-1β, IL-6, and macrophage colony-stimulating factor (M-CSF/CSF-1) [36–41]. Interestingly, while some cellular consequences

of TREM-1 activation such as upregulation of chemokines, cytokines, matrix metalloproteases, and post transcriptional gene silencing (PTGS)/COX2 are similar to those observed upon lipopolysaccharide stimulation, which is consistent with a core inflammatory response, other immunomodulatory factors, including secreted phosphoprotein 1 (SPP1) and M-CSF, are induced selectively in response to TREM-1 cross-linking [38]. In line with these findings, inhibition of TREM-1 in vivo was shown to reduce release of MCP-1, TNFα, IL-1β, IL-6, and M-CSF [28,36,40–44]. Blockade of TREM-1 is a promising approach in a variety of inflammation-associated disorders including sepsis, cancer, rheumatoid arthritis and other serious diseases with unmet clinical needs [28,36,39–41,43–46]. However, despite the recent identification of TREM-1 as a novel hypoxic marker in vivo and in vitro [47], the role of TREM-1 in RNV diseases remains unclear.

In this study, to investigate the role of TREM-1 in the pathogenesis of RNV and its potential as a therapeutic target, we employed the OIR mouse model [17] and our novel, first-in-class TREM-1 inhibitory peptide GF9 [39–41] designed using the signaling chain homooligomerization (SCHOOL) model of TREM-1 signaling [48,49]. In order to improve peptide half-life and its targeted delivery to macrophages, we formulated GF9 into self-assembling lipopeptide complexes that mimic human high density lipoproteins (HDL). In contrast to native HDL, our complexes have two chemically modified peptides with sequences corresponding to those of helices 4 (H4, or PE22) and 6 (H6, or PA22) of the major HDL protein, apolipoprotein (apo) A-I, and deliver the incorporated agents to macrophages [39–41,50,51]. In addition to GF9-HDL, we also used HDL-formulated 31 amino acid-long peptides GE31 and GA31 with combined sequences corresponding to those of GF9 and PE22 and PA22, respectively. By combining these sequences, GA31 and GE31 can perform three functions: assist in the self-assembly of HDL, target HDL to macrophages and inhibit TREM-1 in vivo [40,41].

2. Materials and methods

2.1. Lipopeptide complexes

GF9-loaded HDL-mimicking lipopeptide complexes that contain an equimolar mixture of PE22 and PA22 (GF9-HDL) as well as the complexes that contain an equimolar mixture of GA31 and GE31 (GA/E31-HDL) were synthesized using the sodium cholate dialysis procedure, purified and characterized as previously described [39–41]. In a subset of experiments, 1,2-dimyristoyl-sn-glycero-3-phosphoethanolamine-N(lissamine rhodamine B sulfonyl) was added to reaction mixtures to prepare rhodamine B (rho-B)-labeled GF9-HDL and rho B-labeled GA/E31-HDL as reported [39–41].

2.2. In vitro macrophage uptake

BALB/c murine macrophage J774A.1 cells were obtained from ATCC (Manassas, VA) and cultured according to manufacturer's instructions at 37 °C in 6-well tissue culture plates containing glass coverslips until reaching about 50% confluency. Then, cells were incubated for 6 h at 37 °C either with rho B-labeled GF9-HDL that contained Dylight 488-labeled GF9 and Dylight 405-labeled PE22 or with GA/E31-HDL that contained Dylight 488-labeled GE31. In colocalization experiments, TREM-1 staining was performed using an Alexa 647-

labeled rat anti-mouse TREM-1 antibody (Bio-Rad, Hercules, CA) as previously described [40]. Coverslips were mounted using Prolong Gold anti-fade DAPI (4′,6-diamidino-2-phenylindole) mounting medium. Confocal imaging was performed using a Leica TCS SP5 II laser scanning confocal microscope as reported [40].

2.3. Mouse model of oxygen-induced retinopathy

This study was carried out in strict accordance with the recommendations in the Guide for the Care and Use of Laboratory Animals of the National Institutes of Health and in the United States Department of Agriculture Animal Welfare Act (9 CFR, Parts 1, 2, and 3). All experimental procedures were approved by the Institutional Animal Care and Use Committee at the Augusta University (Animal Welfare Assurance Number A3307–01) and all animals were treated according to the Association for Research in Vision and Ophthalmology Statement for the Use of Animals in Ophthalmic and Vision Research.

Litters of C57BL/6J (Jackson Laboratory, Bar Harbor, ME) neonatal mice and nursing dams were exposed to a hyperoxia environment (75% oxygen) from postnatal day 7 (P7) to P12 and returned to normoxia until P17. The hyperoxia exposure causes degeneration of the immature retinal vessels. This results in severe hypoxia upon return to the normoxia environment which leads to vitreoretinal neovascularization. Beginning on P7, mice were treated until P17 by daily intraperitoneal (i.p.) injections of GF9-HDL, GA/E31-HDL or vehicle (phosphate-buffered saline, pH 7.4; PBS). In a subset of experiments, rho B-labeled GF9-HDL and GA/E31-HDL were used to confirm the ability of these lipopeptide complexes to cross the BRB. In another subset of experiments, neonatal mice and nursing dams were not subjected to a hyperoxia environment and reared in room air (RA). At P17, all mice were humanely sacrificed and their retinas were collected.

2.4. Immunofluorescence staining

Treatment effects on vaso-obliteration and pathological angiogenesis were assessed by morphometric analysis of the avascular and neovascularization areas in retinal flat mounts after labeling with isolectin B_4 as described previously [52,53]. Immunofluorescence analysis (IFA) of the retina flat mounts was performed to assess the effects of the TREM-1-targeting treatments on the distribution of TREM-1, M-CSF and markers for inflammatory cells (CD45) and activated macrophage/microglial cells (Iba-1) in relation to RNV. Retinal frozen sections from pups kept in RA and from the OIR pups were fixed in 4% paraformaldehyde for 15 min (or in cold acetone at −20 °C for 30 min), washed 3 times with PBS, and blocked with a solution containing 0.3% Triton X and 3% normal goat serum (NGS) for 30 min. Then, the samples were reacted with a rat anti-mouse TREM-1 antibody (Abcam, Cambridge, MA), rabbit polyclonal anti-mouse M-CSF antibodies (Abcam, Cambridge, MA), rabbit polyclonal anti-mouse CD45 antibodies (Santa Cruz Biotechnology, Dallas, TX), a rabbit anti-mouse Iba1 antibody (Wako Chemical USA, Inc.), and kept at 4°C overnight. Then, the samples were washed 3 times with PBS and stained with a donkey anti-rat Oregon Green antibody for TREM-1, a goat anti-rabbit Texas Red antibody for CD45 and Iba-1 or a donkey anti-rabbit Texas Red antibody for M-CSF (Invitrogen, Waltham, MA). After washing 3 times with PBS, the images were captured with a 20× lens using a Zeiss Axioplan2 fluorescence microscope (Carl Zeiss Meditec, Inc.,

Dublin, CA). Intravitreal neovascular formation and avascular areas were measured as described [54].

2.5. Western blot analysis

Retina samples from OIR and RA control pups were homogenized in modified RIPA buffer (20 mM Tris-HCl, 2.5 mM EDTA, 50 mM NaF, 10 mM $Na_4P_2O_7$, 1% Triton X-100, 0.1% sodium dodecyl sulfate, 1% sodium deoxycholate, 1 mM phenyl methyl sulfonyl fluoride, pH 7.4). Samples containing equal amounts of protein were separated by 12% sodium dodecyl sulfate polyacrylamide gel electrophoresis, transferred to nitrocellulose membrane, and reacted for 24 h with monoclonal rat anti-mouse TREM-1 or polyclonal rabbit M-CSF antibodies (Abcam, Cambridge, MA) in 5% milk, followed by incubation with corresponding horseradish peroxidase-linked secondary antibodies (GE Healthcare Bio-Science Corp., Piscataway, NJ). Bands were quantified by densitometry, and the data were analyzed using Image Studio Lite software and normalized to loading control. Equal loading was verified by stripping the membranes and reprobing them with a monoclonal antibody against β-actin (Sigma-Aldrich, St Louis, MO).

2.6. Statistical analysis

Group differences were compared by one-way ANOVA followed with a post hoc test for multiple comparisons. Values are represented as the means ± standard error of the means (SEM). Results were considered statistically significant when $p < 0.05$.

3. Results

3.1. Induction of TREM-1 in OIR

To investigate the expression of TREM-1 associated with the development of pathological RNV, we used Western blot analysis to examine the retinas of OIR mice and RA control mice on P17. High levels of TREM-1 were observed in the OIR samples, while no detectable TREM-1 expression was observed in the RA control samples (Fig. 1A). IFA showed that in the retinas of OIR mice at P17, TREM-1 is largely colocalized with M-CSF that is also overexpressed in OIR (Fig. 1B). Further, IFA of retinal cryosections from OIR mice at P17 demonstrated localization of TREM-1 in pathological retinal neovessels positive for the vascular endothelial cell/macrophage marker isolectin B_4 (Fig. 2A), the leukocyte marker CD45 (Fig. 2B), the microglia/macrophage marker Iba-1 (Fig. 2C), and M-CSF (Fig. 2D). Comparatively, the RA samples were immunostained for CD45 and Iba-1 and studied by IFA (Supplemental Fig. 1A,B). Collectively, these findings indicate that TREM-1 is highly upregulated during pathological but not physiological RNV and this upregulation is accompanied by induction of M-CSF.

3.2. Targeted delivery of TREM-1 inhibitory peptides

To further investigate the mechanisms of macrophage-targeted delivery of TREM-1 inhibitory peptides, we designed the GF9, GA31 and GE31 peptides using the SCHOOL model of TREM-1 signaling (Fig. 3A) and formulated these peptides into HDL-mimicking lipopeptide complexes (GF9-HDL and GA/E31-HDL, respectively). To rule out nonspecific cell surface binding and to confirm intracellular uptake of the entire GF9-HDL complex, we

incubated J774 macrophages with GF9-HDL containing rho B-labeled lipid, Dylight 488-labeled GF9 and Dylight 405-labeled oxidized apo A-I peptide PE22. We observed intracellular localization of GF9 as well as both lipid and apo A-I peptide constituents of HDL (Fig. 3B), suggesting that the entire GF9-HDL complex is intracellularly endocytosed by macrophages, most likely through a scavenger receptor-mediated mechanism. By using GA/E31-HDL that contained Dylight 488-labeled GE31, we demonstrated that similarly to GF9 [40], the intracellularly delivered trifunctional peptide GE31 (and likely GA31) self-penetrates into the cell membrane from inside the cell and colocalizes with TREM-1 (Fig. 3C).

3.3. TREM-1 blockade reduces pathological retinal neovascularization

To evaluate pathological RNV in OIR mice, we analyzed retinal flat-mounts at P17 using IFA and anti-isolectin B_4 antibodies and demonstrated excessive pathological vessel growth detected in the superficial plexus of vehicle-treated retina of the OIR mice (Fig. 4A). This was accompanied by the formation of a large avascular area in the central retina, with only the major vessels present and practically no capillary network (Fig. 4A). When i.p. administered at a dose of 2.5 mg of GF9/kg, GF9-HDL reduced RNV by at least 95% compared with vehicle treatment (Fig. 4A,B). Similar anti-angiogenic activity was observed for GA/E31-HDL i.p. administered at a dose equivalent to 4 mg of GF9/kg (Fig. 4A,B). The reduced central avascular area was observed for both formulations (Fig. 4A,C). These results demonstrate that the TREM-1 inhibitors used in this study have strong anti-angiogenic effects on pathological RNV while allowing physiological neovascularization.

Confocal analysis revealed the presence of rho B fluorescence in the retinas of the OIR mice i.p. administered with rho B-labeled HDL that contained either GF9 (GF9-HDL, Fig. 4D) or an equimolar mixture of GA31 and GE31 (GA/E31-HDL, Supplemental Fig. 1C) further confirming that the self-assembling HDL-mimicking complexes used in the present study are able to pass the BRB and deliver their cargo to the retina.

3.4. Downregulation of TREM-1 and M-CSF by TREM-1 inhibitors

To further evaluate the molecular mechanisms of the anti-angiogenic activity of TREM-1-specific peptide inhibitors, we measured TREM-1 and M-CSF protein levels at the peak of pathological RNV (P17). Western blot analysis indicated that expression of TREM-1 and M-CSF was substantially decreased in OIR mice systemically treated with 2.5 mg/kg GF9-HDL or 4 mg/kg GA/E31-HDL as compared with those observed in the vehicle-treated OIR mice (Fig. 5). These results further confirm that the anti-angiogenic mechanisms of TREM-1-targeted treatment involve inhibiting the TREM-1 signaling pathway, which is accompanied by downregulation of M-CSF.

4. Discussion

To the best of our knowledge, this study is the first to demonstrate the role of TREM-1 in pathological RNV and implicate this receptor as a novel promising therapeutic target in retinal diseases characterized by pathological RNV. TREM-1 levels were significantly increased in retinas of mice exposed to OIR as compared to those of the room air control

group (Fig. 1A). Interestingly, increased TREM-1 levels were accompanied by induction of M-CSF (Fig. 1B), which is known to play a role in angiogenesis [12], and both were found to be largely colocalized in OIR (Fig. 1B). M-CSF is required for the differentiation of tissue macrophages and microglia during postnatal development [55]. In animal models of breast cancer, M-CSF has been shown to act as an “angiogenic switch” [56]. Continuous inhibition of M-CSF suppresses tumor angiogenesis and growth [12,57], while healthy vascular and lymphatic systems outside tumors remain unaffected [12]. It has been reported that M-CSF induces VEGF production and angiogenic activity by cultured monocytes [58]. In contrast to VEGF blockade, interruption of M-CSF inhibitory treatment does not promote rapid vascular regrowth [12]. In OIR mice, M-CSF is required for pathological RNV but not for the recovery of normal vasculature [12]. In line with these findings, in the retinas of diabetic rats and in the vitreous of patients with proliferative DR, M-CSF levels are significantly higher as compared with those of control subjects [59,60]. This suggests targeting M-CSF either directly or via the specific inflammatory signaling pathway as a highly promising strategy for treating ocular neovascular diseases including ROP.

The role of TREM-1 in pathological but not physiological RNV is further supported by the observation that upregulated TREM-1 is localized in pathological retinal neovessels positive for isolectin B_4, CD45 (Fig. 2B), Iba-1 (Fig. 2C), or M-CSF (Fig. 2D). This suggests that activated microglia/macrophages are the main source of TREM-1 expression in the retinas of OIR mice and that TREM-1 plays a role in RNV progression, likely through a mechanism that involves M-CSF. Collectively, these data strongly implicate TREM-1 as a potential therapeutic target for RNV diseases.

Previously, we used TREM-1 inhibitory GF9 peptide sequences that employ the SCHOOL mechanisms of TREM-1 blockade (Fig. 3A) in order to silence the specific TREM-1-mediated signaling pathway in cancer, sepsis, and rheumatoid arthritis [39–41]. According to the SCHOOL model of TREM-1 signaling [48,49], GF9 self-penetrates into the cell membrane and disrupts intramembrane interactions between TREM-1 and DAP-12 (Fig. 3A). In this study, we used GF9, GA31 and GE31 peptide inhibitors of TREM-1 formulated into macrophage-targeted self-assembling lipopeptide complexes. This has been previously shown to extend peptide half-life and substantially (up to 10-fold) decrease the effective peptide therapeutic dose in cancer [39,41] and arthritic mice [40]. Notably, formulation of GF9 into macrophage-specific complexes GF9-HDL results in intracellular delivery of all lipid and peptide (both GF9 and apo A-I) constituents to macrophages (Fig. 3B), suggesting endocytosis of the entire GF9-HDL complex, most likely in a receptor-mediated manner. Our previous and current data also indicate that as hypothesized (Fig. 3A), upon delivery into macrophages, similarly to the short-chain peptide GF9 [40], the 31 amino acid-long trifunctional peptides are able to reach their intramembrane site of action from inside the cell and colocalize with TREM-1 in the cell membrane (Fig. 3C). Further, using confocal microscopy, we found that similarly to native HDL [61,62], HDL-like lipopeptide complexes containing TREM-1 inhibitory SCHOOL peptides are able to pass the blood-brain barrier (Zu T. Shen and Alexander B. Sigalov; unpublished results). In this study, we demonstrate that these complexes can also infiltrate BRB as shown for both GF9-HDL (Fig. 4D) and GA/E31-HDL (Supplemental Fig. 1C). It should be noted here that drug delivery to the retina via

systemic administration is ideal for patients with ROP but remains a challenge due to the BRB [63].

The high efficacy of systemically administered TREM-1 inhibitory formulations in reducing up to 95% of pathological but not physiological angiogenesis in OIR demonstrated in our study (Fig. 4) further implicates TREM-1 as one of the key players in the development of pathological vitreoretinal neovascularization and as a novel target in the treatment of RNV disorders. Interestingly, our current observations that TREM-1 blockade is accompanied by a significant reduction of M-CSF protein expression in the retina (Fig. 5) strongly correlate with our previous studies, which demonstrated that blockade of TREM-1 reduced serum levels of M-CSF in arthritic [40] and cancer [41] mice, further supporting the idea that TREM-1 signaling promotes the M-CSF-mediated involvement in angiogenesis that is observed in the present study. One can suggest that reduction of M-CSF resulting from TREM-1 inhibition can represent a mechanistic link between the previously shown anticancer and anti-arthritic activities of TREM-1-specific SCHOOL inhibitory peptides [39–41] and their ability to prevent RNV in OIR demonstrated in the present study. Further studies are required to determine the effects of inhibiting TREM-1 on VEGF expression in the OIR model.

In summary, our study for the first time, reveals an important role of TREM-1 in the development of pathological RNV. Down-regulation of TREM-1 and silencing the TREM-1 signaling pathway using novel, first-in-class TREM-1 blockers effectively inhibited RNV and improved normal vascularization in the OIR mouse model. Furthermore, in retinopathy, like other inflammatory disorders where blockade of TREM1 has beneficial effect on disease prevention and management, M-CSF is likely to be involved in the underlying molecular mechanisms associated with the pathological RNV process.

Importantly, formulation of TREM-1 inhibitory GF9 peptide sequences into HDL-mimicking macrophage-specific lipopeptide complexes that are able to pass the BRB allows for their systemic administration with low toxicity. Another important consideration is that the actual nature of the TREM-1 ligand(s) is still unknown, which increases the risk for failure in the clinical development of current approaches that all attempt to block the binding of TREM-1 to its ligand(s) [28,36,45,64]. Advantageously, first-in-class TREM-1-specific SCHOOL inhibitory peptides employ a new, ligand-independent mechanism of TREM-1 blockade [39–41], which avoids this risk. It should be also noted that TREM-1 blockade does not affect microbial control [65] and was suggested for the treatment of neonatal infection [66]. Moreover, septic mice lacking DAP12, a signaling adapter of TREM-1, have improved survival [67]. Humans lacking DAP12 do not have problems resolving infections [68]. In future studies, we will determine the possible effects of TREM-1 blockade on normal development. However, our current study showed no changes in weight gain or behavior of the neonatal mice treated with the TREM-1 inhibitors.

Collectively, these promising data suggest that targeting TREM-1 using TREM-1-specific SCHOOL peptide inhibitors represents a novel strategy to prevent the development of pathological RNV during ROP or other retinal diseases characterized by vitreoretinal neovascularization.

Supplementary Material

Refer to Web version on PubMed Central for supplementary material.

Acknowledgments

Financial support

This work was partly supported by the National Cancer Institute of the National Institutes of Health grant R43CA195684 (ZTS, ABS; Alexander B. Sigalov, Principal Investigator) and the National Eye Institute of the National Institutes of Health grant R43EY028779 (ZTS, ABS; Alexander B. Sigalov, Principal Investigator), the National Eye Institute of the National Institutes of Health grant R01EY11766 (Ruth B. Caldwell, Principal Investigator), and the Vision Discovery Institute grant 70000–15000-04340046–12100-11200 (Modesto A. Rojas, Principal Investigator). Ruth B. Caldwell is the recipient of a Research Career Scientist Award from the Department of Veterans Affairs. The additional funding (ABS, MAR, ZTS) has come from SignaBlok, Inc. The sponsors were not involved in the study design, data collection, analysis and interpretation and the writing of the report.

References

[1]. Jo DH, Kim JH, Arch. Pharm. Res 33 (2010) 1557–1565. [PubMed: 21052933]

[2]. Aiello LP, Avery RL, Arrigg PG, Keyt BA, Jampel HD, Shah ST, Pasquale LR, Thieme H, Iwamoto MA, Park JE, et al. N. Engl. J. Med 331 (1994) 1480–1487. [PubMed: 7526212]

[3]. Laouri M, Chen E, Looman M, Gallagher M, Eye 25 (2011) 981–988. [PubMed: 21546916]

[4]. Mutlu FM, Sarici SU, Int. J. Ophthalmol 6 (2013) 228–236. [PubMed: 23641347]

[5]. Al-Shabrawey M, Elsherbiny M, Nussbaum J, Othman A, Megyerdi S, Tawfik A, Expert Rev. Ophthalmol 8 (2013) 267–286. [PubMed: 25598837]

[6]. Bashinsky AL, N. C. Med. J 78 (2017) 124–128. [PubMed: 28420777]

[7]. Hartnett ME, Surv. Ophthalmol 62 (2017) 257–276. [PubMed: 28012875]

[8]. Pieramici DJ, Rabena MD, Eye 22 (2008) 1330–1336. [PubMed: 18497829]

[9]. Maharaj AS, Walshe TE, Saint-Geniez M, Venkatesha S, Maldonado AE, Himes NC, Matharu KS, Karumanchi SA, D'Amore PA, J. Exp. Med 205 (2008) 491–501. [PubMed: 18268040]

[10]. Verheul HM, Pinedo HM, Nat. Rev. Cancer 7 (2007) 475–485. [PubMed: 17522716]

[11]. Mancuso MR, Davis R, Norberg SM, O'Brien S, Sennino B, Nakahara T, Yao VJ, Inai T, Brooks P, Freimark B, Shalinsky DR, Hu-Lowe DD, McDonald DM, J. Clin. Invest 116 (2006) 2610–2621. [PubMed: 17016557]

[12]. Kubota Y, Takubo K, Shimizu T, Ohno H, Kishi K, Shibuya M, Saya H, Suda T, J. Exp. Med 206 (2009) 1089–1102. [PubMed: 19398755]

[13]. Checchin D, Sennlaub F, Levavasseur E, Leduc M, Chemtob S, Invest. Ophthalmol. Vis. Sci 47 (2006) 3595–3602. [PubMed: 16877434]

[14]. Espinosa-Heidmann DG, Suner IJ, Hernandez EP, Monroy D, Csaky KG, Cousins SW, Invest. Ophthalmol. Vis. Sci 44 (2003) 3586–3592. [PubMed: 12882811]

[15]. Sakurai E, Anand A, Ambati BK, van Rooijen N, Ambati J, Invest. Ophthalmol. Vis. Sci 44 (2003) 3578–3585. [PubMed: 12882810]

[16]. Akiyama R, Usui T, Yamagami S, Cornea 34 (Suppl. 11) (2015) S115–20. [PubMed: 26448168]

[17]. Smith LE, Wesolowski E, McLellan A, Kostyk SK, D'Amato R, Sullivan R, D'Amore PA, Invest. Ophthalmol. Vis. Sci 35 (1994) 101–111. [PubMed: 7507904]

[18]. Davies MH, Eubanks JP, Powers MR, Mol. Vis 12 (2006) 467–477. [PubMed: 16710171]

[19]. Penfold PL, Madigan MC, Gillies MC, Provis JM, Prog. Retin. Eye Res 20 (2001) 385–414. [PubMed: 11286898]

[20]. Caicedo A, Espinosa-Heidmann DG, Pina Y, Hernandez EP, Cousins SW, Exp. Eye Res 81 (2005) 38–47. [PubMed: 15978253]

[21]. Gao X, Wang YS, Li XQ, Hou HY, Su JB, Yao LB, Zhang J, Cell Tissue Res. 364 (2016) 599–610. [PubMed: 26841878]

[22]. Liu J, Copland DA, Horie S, Wu WK, Chen M, Xu Y, Morgan B. Paul, Mack M, Xu H, Nicholson LB, Dick AD, PLoS One 8 (2013) e72935. [PubMed: 23977372]

[23]. Niu J, Azfer A, Zhelyabovska O, Fatma S, Kolattukudy PE, J. Biol. Chem 283 (2008) 14542–14551. [PubMed: 18364357]

[24]. Nagai A, Nakagawa E, Hatori K, Choi HB, McLarnon JG, Lee MA, Kim SU, Neurobiol. Dis 8 (2001) 1057–1068. [PubMed: 11741401]

[25]. Yoshida S, Yoshida A, Ishibashi T, Elner SG, Elner VM, J. Leukoc. Biol 73 (2003) 137–144. [PubMed: 12525571]

[26]. Kim MY, Byeon CW, Hong KH, Han KH, Jeong S, FEBS Lett. 579 (2005) 1597–1601. [PubMed: 15757647]

[27]. Bouchon A, Dietrich J, Colonna M, J. Immunol 164 (2000) 4991–4995. [PubMed: 10799849]

[28]. Bouchon A, Facchetti F, Weigand MA, Colonna M, Nature 410 (2001) 1103–1107. [PubMed: 11323674]

[29]. Bleharski JR, Kiessler V, Buonsanti C, Sieling PA, Stenger S, Colonna M, Modlin RL, J. Immunol 170 (2003) 3812–3818. [PubMed: 12646648]

[30]. Tessarz AS, Cerwenka A, Immunol. Lett 116 (2008) 111–116. [PubMed: 18192027]

[31]. Klesney-Tait J, Turnbull IR, Colonna M, Nat. Immunol. 7 (2006) 1266–1273. [PubMed: 17110943]

[32]. Colonna M, Facchetti F, J. Infect. Dis 187 (Suppl. 2) (2003) S397–401. [PubMed: 12792857]

[33]. Gonzalez-Roldan N, Ferat-Osorio E, Aduna-Vicente R, Wong-Baeza I, EsquivelCallejas N, Astudillo-de la Vega H, Sanchez-Fernandez P, Arriaga-Pizano L, Villasis-Keever MA, Lopez-Macias C, Isibasi A, World J Gastroenterol. 11 (2005) 7473–7479.

[34]. Koussoulas V, Vassiliou S, Demonakou M, Tassias G, Giamarellos-Bourboulis EJ, Mouktaroudi M, Giamarellou H, Barbatzas C, Eur. J. Gastroenterol. Hepatol 18 (2006) 375–379. [PubMed: 16538108]

[35]. Wang DY, Qin RY, Liu ZR, Gupta MK, Chang Q, World J Gastroenterol. 10 (2004) 2744–2746.

[36]. Schenk M, Bouchon A, Seibold F, Mueller C, J. Clin. Invest 117 (2007) 3097–3106. [PubMed: 17853946]

[37]. Lagler H, Sharif O, Haslinger I, Matt U, Stich K, Furtner T, Doninger B, Schmid K, Gattringer R, de Vos AF, Knapp S, J. Immunol 183 (2009) 2027–2036. [PubMed: 19596984]

[38]. Dower K, Ellis DK, Saraf K, Jelinsky SA, Lin LL, J. Immunol 180 (2008) 3520–3534. [PubMed: 18292579]

[39]. Sigalov AB, Int. Immunopharmacol 21 (2014) 208–219. [PubMed: 24836682]

[40]. Shen ZT, Sigalov AB, J. Cell. Mol. Med 21 (2017) 2524–2534. [PubMed: 28382703]

[41]. Shen ZT, Sigalov AB, Mol. Pharm 14 (2017) 4572–4582. [PubMed: 29095622]

[42]. Sigalov AB, Int. Immunopharmacol 21 (2014) 208–219. [PubMed: 24836682]

[43]. Gibot S, Massin F, Alauzet C, Montemont C, Lozniewski A, Bollaert PE, Levy B, Crit. Care Med 36 (2008) 504–510. [PubMed: 18091551]

[44]. Luo L, Zhou Q, Chen XJ, Qin SM, Ma WL, Shi HZ, Chin. Med. J 123 (2010) 1561–1565. [PubMed: 20819512]

[45]. Murakami Y, Akahoshi T, Aoki N, Toyomoto M, Miyasaka N, Kohsaka H, Arthritis Rheum. 60 (2009) 1615–1623. [PubMed: 19479878]

[46]. Gibot S, Massin F, Alauzet C, Derive M, Montemont C, Collin S, Fremont S, Levy B, Shock 32 (2009) 633–637. [PubMed: 19333144]

[47]. Bosco MC, Pierobon D, Blengio F, Raggi F, Vanni C, Gattorno M, Eva A, Novelli F, Cappello P, Giovarelli M, Varesio L, Blood 117 (2011) 2625–2639. [PubMed: 21148811]

[48]. Sigalov AB, Trends Immunol. 25 (2004) 583–589. [PubMed: 15489186]

[49]. Sigalov AB, Trends Pharmacol. Sci 27 (2006) 518–524. [PubMed: 16908074]

[50]. Shen ZT, Zheng S, Gounis MJ, Sigalov AB, PLoS One 10 (2015) e0143453. [PubMed: 26569115]

[51]. Sigalov AB, Contrast Media Mol. Imaging 9 (2014) 372–382. [PubMed: 24729189]

[52]. Al-Shabrawey M, Bartoli M, El-Remessy AB, Platt DH, Matragoon S, Behzadian MA, Caldwell RW, Caldwell RB, Am. J. Pathol 167 (2005) 599–607. [PubMed: 16049343]

[53]. Patel C, Narayanan SP, Zhang W, Xu Z, Sukumari-Ramesh S, Dhandapani KM, Caldwell RW, Caldwell RB, Am. J. Pathol 184 (2014) 3040–3051. [PubMed: 25203536]

[54]. Connor KM, Krah NM, Dennison RJ, Aderman CM, Chen J, Guerin KI, Sapieha P, Stahl A, Willett KL, Smith LE, Nat. Protoc 4 (2009) 1565–1573. [PubMed: 19816419]

[55]. Cecchini MG, Dominguez MG, Mocci S, Wetterwald A, Felix R, Fleisch H, Chisholm O, Hofstetter W, Pollard JW, Stanley ER, Development 120 (1994) 1357–1372. [PubMed: 8050349]

[56]. Lin EY, Li JF, Gnatovskiy L, Deng Y, Zhu L, Grzesik DA, Qian H, Xue XN, Pollard JW, Cancer Res. 66 (2006) 11238–11246. [PubMed: 17114237]

[57]. Aharinejad S, Paulus P, Sioud M, Hofmann M, Zins K, Schafer R, Stanley ER, Abraham D, Cancer Res. 64 (2004) 5378–5384. [PubMed: 15289345]

[58]. Eubank TD, Galloway M, Montague CM, Waldman WJ, Marsh CB, J. Immunol 171 (2003) 2637–2643. [PubMed: 12928417]

[59]. Yoshida S, Kobayashi Y, Nakama T, Zhou Y, Ishikawa K, Arita R, Nakao S, Miyazaki M, Sassa Y, Oshima Y, Izuhara K, Kono T, Ishibashi T, Br. J. Ophthalmol 99 (2015) 629–634. [PubMed: 25355804]

[60]. Liu W, Xu GZ, Jiang CH, Da CD, Curr. Eye Res 34 (2009) 123–133. [PubMed: 19219684]

[61]. Wang H, Eckel RH, Trends Endocrinol. Metab 25 (2014) 8–14. [PubMed: 24189266]

[62]. Zheng W, Reem RE, Omarova S, Huang S, DiPatre PL, Charvet CD, Curcio CA, Pikuleva IA, PLoS One 7 (2012) e37926. [PubMed: 22629470]

[63]. Gaudana R, Ananthula HK, Parenky A, Mitra AK, AAPS J 12 (2010) 348–360. [PubMed: 20437123]

[64]. Derive M, Boufenzer A, Gibot S, Anesthesiology 120 (2014) 935–942. [PubMed: 24270127]

[65]. Weber B, Schuster S, Zysset D, Rihs S, Dickgreber N, Schurch C, Riether C, Siegrist M, Schneider C, Pawelski H, Gurzeler U, Ziltener P, Genitsch V, Tacchini-Cottier F, Ochsenbein A, Hofstetter W, Kopf M, Kaufmann T, Oxenius A, Reith W, Saurer L, Mueller C, PLoS Pathog. 10 (2014) e1003900. [PubMed: 24453980]

[66]. Qian L, Weng XW, Chen W, Sun CH, Wu J, Int. J. Clin. Exp. Med 7 (2014) 1650–1658. [PubMed: 25126161]

[67]. Turnbull IR, McDunn JE, Takai T, Townsend RR, Cobb JP, Colonna M, J. Exp. Med 202 (2005) 363–369. [PubMed: 16061725]

[68]. Lanier LL, Immunol. Rev 227 (2009) 150–160. [PubMed: 19120482]

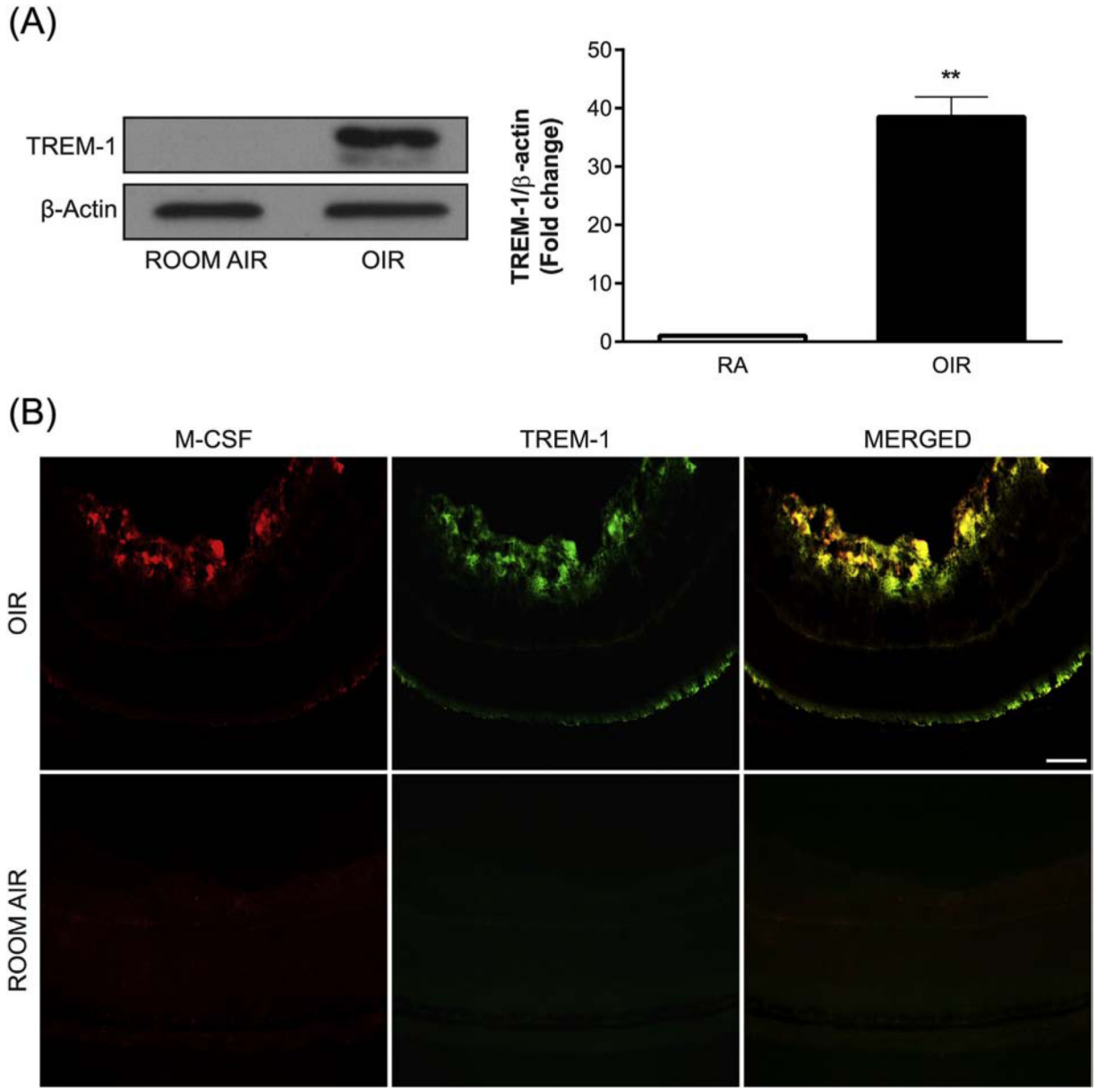

Fig. 1.

OIR induces TREM-1 and M-CSF expression. (A) A representative Western blot shows TREM-1 expression at P17 in the retinas of OIR mice but not of those kept in room air (RA). The membrane was probed for TREM-1 and then reprobed for β-actin. Values in the bar graphs represent the mean ± SEM, n = 5. **, $p < 0.01$ vs. RA mice. (B) Representative retinal cryosections from OIR and RA mice at P17 were immunolabeled with antibodies against M-CSF (red) and TREM-1 (green). TREM-1 and M-CSF are induced and largely colocalized in OIR. Scale bar = 20 μm. Five retinas were analyzed for each experimental group.

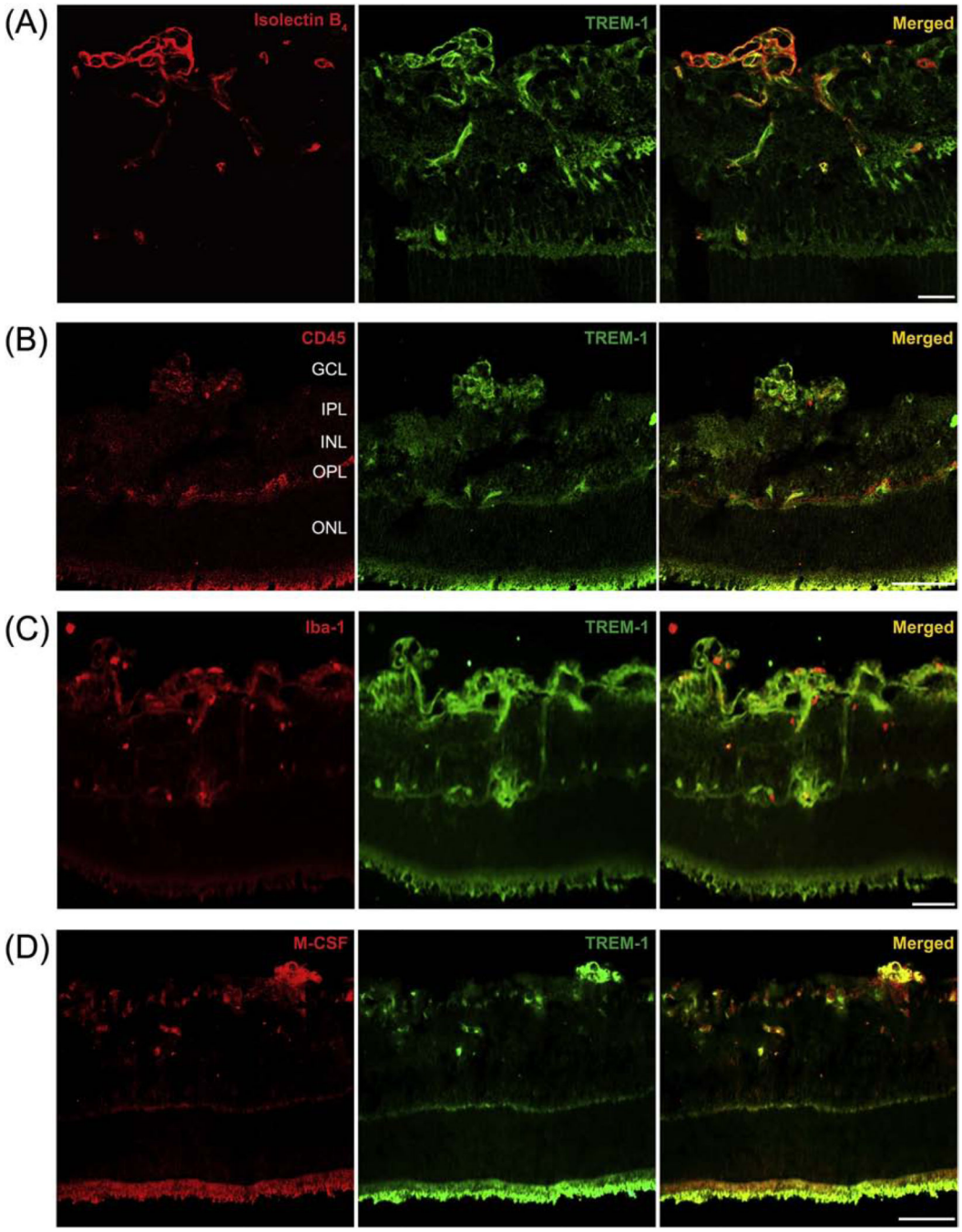

Fig. 2.

TREM-1 colocalizes with activated microglia and macrophages in pathological retinal neovessels. Representative retinal cryosections from OIR mice at P17 were immunolabeled with antibodies against TREM-1 (green, A-D), the endothelial cell/macrophage marker isolectin B_4 (red, A), the leukocyte marker CD45 (red, B), the macrophage/microglial marker Iba-1 (red, C), and M-CSF (red, D). The merged images (A-D) demonstrate that TREM-1 localizes to pathological retinal neovessels, largely colocalizing with isolectin B_4,

CD45, Iba-1 and M-CSF. GCL, ganglion cell layer; IPL, inner plexiform layer; INL, inner nuclear layer; OPL, outer plexiform layer; ONL, outer nuclear layer. Scale bar = 20 μm.

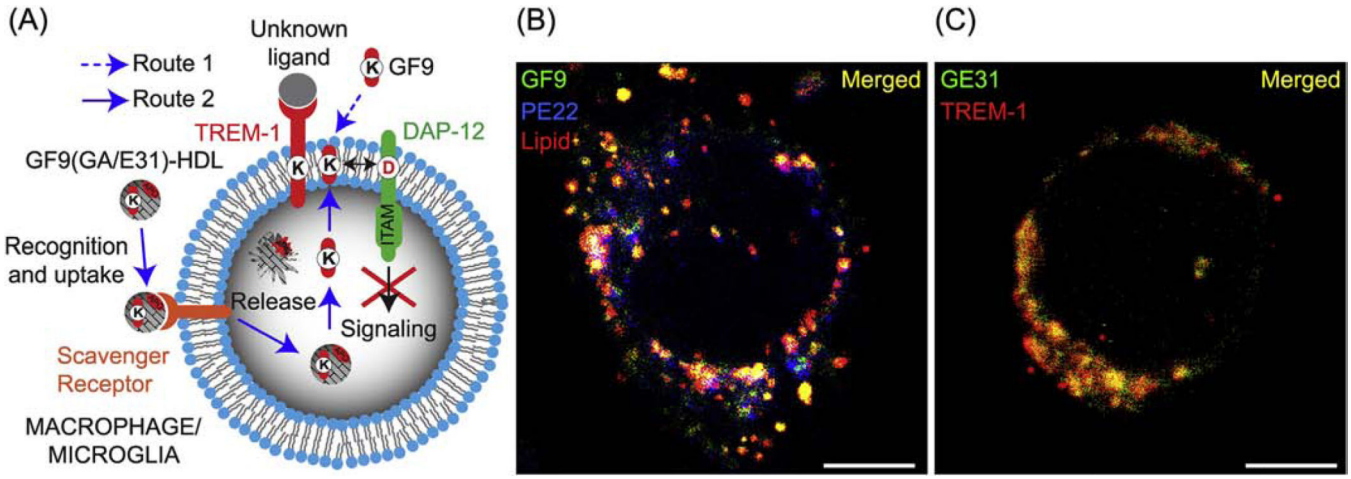

Fig. 3.

First-in-class peptide inhibitors employ novel mechanisms of action to inhibit TREM-1 signaling. (A) TREM-1 inhibitory GF9 peptide sequences employ ligandindependent (SCHOOL) mechanisms of action and block intramembrane interactions between TREM-1 and its signaling partner DAP-12. These peptides can be employed as free (Route 1) or bound to HDL-mimicking lipopeptide complexes for targeted delivery to macrophages/ microglia (Route 2). (B) Immunofluorescence analysis (IFA) of TREM-1-expressing J774A. 1 macrophages incubated for 6 h at 37 °C with rhodamine B-labeled GF9-HDL that contain Dylight 488-labeled GF9 (green) and Dylight 405-labeled PE22 (blue) demonstrates intracellular delivery of GF9 as well as both lipid and apo A-I peptide constituents of HDL complexes. Scale bar = 5 μm. (C) IFA of TREM-1-expressing J774A.1 macrophages incubated for 6 h at 37 °C with GA/E31-HDL that contain Dylight 488-labeled GE31 (green) and stained using Alexa 647-labeled anti-TREM-1 antibody (red) demonstrates colocalization of GE31 with TREM-1 in the cell membrane. Scale bar = 5 μm.

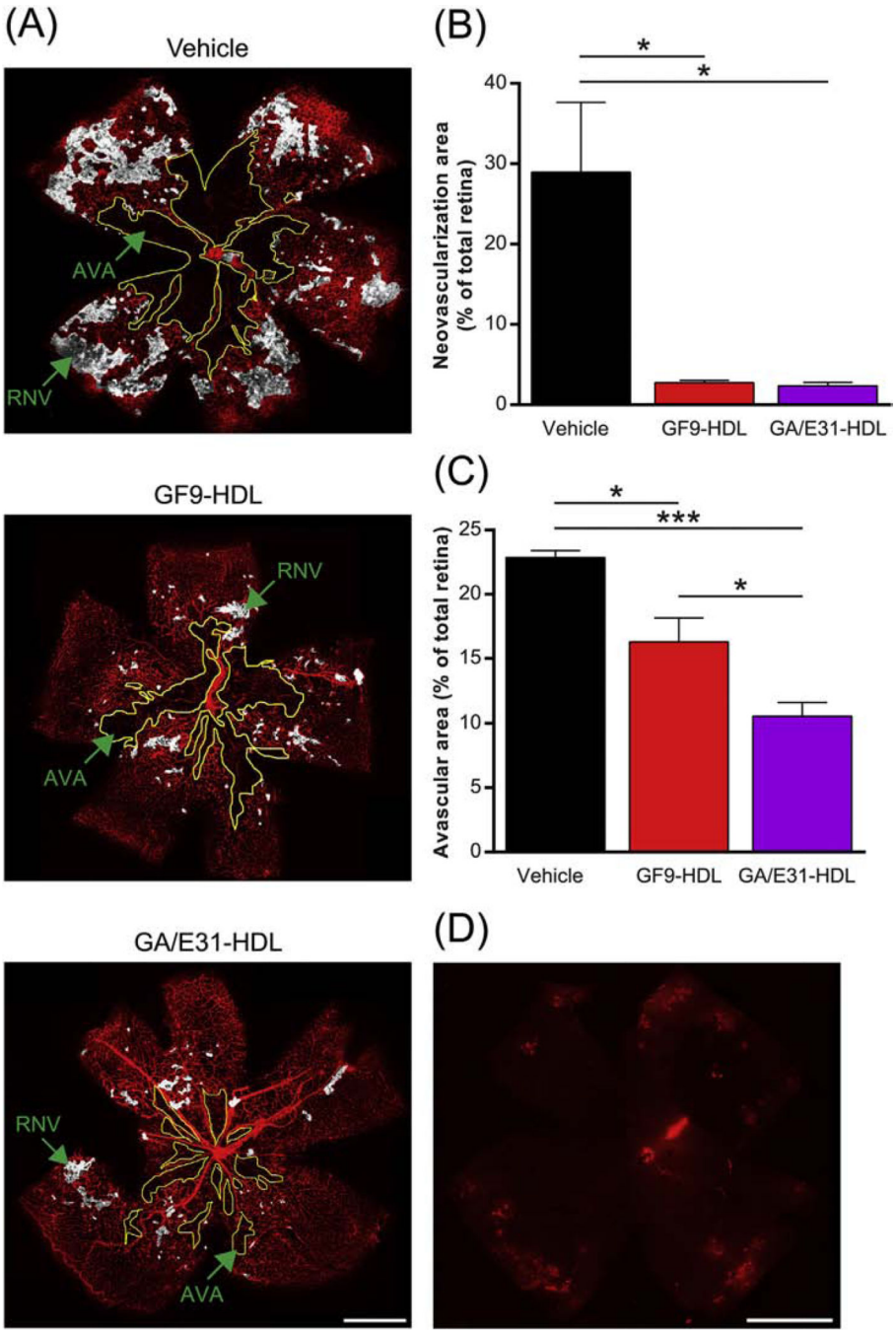

Fig. 4.

TREM-1 blockade reduces pathological retinal neovascularization and avascular areas in OIR. As described in the methods, OIR mice were treated by daily intraperitoneal (i.p.) injections of GF9-HDL (2.5 mg/kg), GA/E31-HDL (4 mg/kg) or vehicle (PBS) from P7 to P17. (A) Representative retina flat-mounts at P17 stained using isolectin B_4 (red) from the indicated treatment groups. Regions of retinal neovascularization (RNV) and avascular areas (AVA) are indicated. Scale bar = 500 μm. (B) Quantification of RNV. Data were analyzed from 3 independent experiments (n = 6 retinas, 3 litters of mice) and represented as the mean

± SEM. *, $p < 0.05$. (C) Quantification of AVA. Data were analyzed from 3 independent experiments (n = 6 retinas, 3 litters of mice) and represented as the mean ± SEM. *, $p < 0.05$, ***, $p < 0.001$. (D) IFA of a representative retina flat-mount confirms that systemically (i.p.) administered rhodamine B-labeled GF9-HDL penetrate the blood-retinal barrier and accumulate in the retina, delivering their payload (similar for GA/GE31-HDL, as shown in Supplemental Fig. 1C). Scale bar = 500 μm.

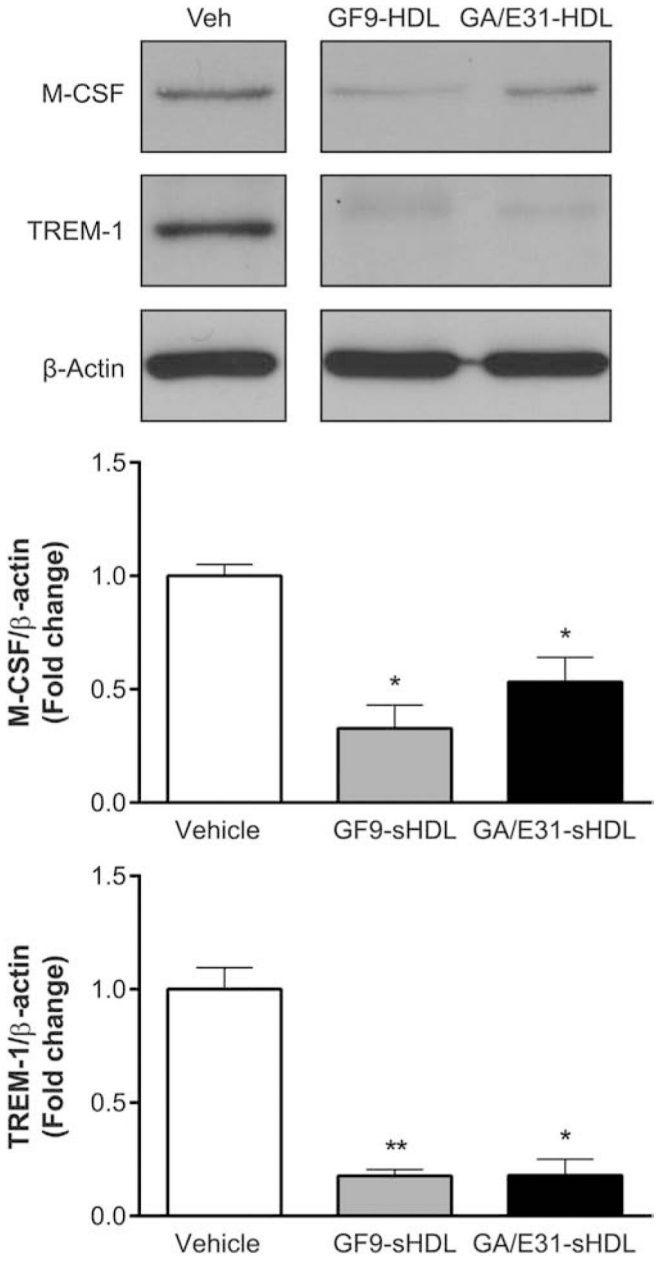

Fig. 5.

TREM-1 inhibition reduces expression of M-CSF and TREM-1 in OIR. A representative Western blot of retinal lysates from OIR mice at P17 reveals that TREM-1 blockade using GF9-HDL and GA/E31-HDL significantly suppresses expression of TREM-1 and M-CSF. The membrane was probed for TREM-1, reprobed for M-CSF and then for β-actin. Values in the bar graphs represent the mean ± SEM, n = 6. *, $p < 0.05$, **, $p < 0.01$ vs. vehicle-treated mice.